

Value of Communication: Data-Driven Topology Optimization for Distributed Linear Cyber-Physical Systems

Michael Nestor^{1*} and Fei Teng¹

¹ Department of Electrical and Electronic Engineering, Imperial College London, UK
m.nestor22@imperial.ac.uk

Abstract. Communication topology is a crucial part of a distributed control implementation for cyber-physical systems, yet is typically treated as a constraint within control design problems rather than a design variable. We propose a data-driven method for designing an optimal topology for the purpose of distributed control when a system model is unavailable or unaffordable, via a mixed-integer second-order conic program. The approach demonstrates improved control performance over random topologies in simulations and efficiently drops links which have a small effect on predictor accuracy, which we show correlates well with closed-loop control cost.

Keywords: communication topology, data-driven control, cyber-physical systems

1 Introduction

1.1 Context and Motivation

The communication topology and its impact on control performance is an emerging topic within the field of distributed control. Distinguished from centralized control, where all local agents must communicate with the central control agent, and decentralized control, where there is no communication at all, distributed control of interconnected dynamical systems has the flexibility to design which agents each agent should send information to or receive information from, even during run time given the increasing reconfigurability of communication solutions, such as software-defined networks. A higher degree of connectivity in the communication graph will improve control performance as each agent has a better picture of the global system, but will lead to increased communication overheads. This paper focuses on how to balance these competing objectives of minimizing communication whilst achieving satisfactory control performance.

Distributed control that achieves cooperation through communication has been proposed as offering better performance than decentralized schemes whilst providing improved flexibility, privacy and computational efficiency compared

*Corresponding author

to centralized control [10]. Consider the example of power distribution grids; significant growth of distributed energy resources such as electric vehicles will require coordination to provide grid services and avoid violating grid constraints. A distributed control structure mirrors the distributed nature of these resources, with the potential for enhanced flexibility and cooperation between, e.g., virtual power plant operators or prosumer communities [18].

There must be a defined scheme for information exchange between agents in order to implement distributed control. All-to-all communication may be optimal from a control perspective, but is likely to lead to prohibitive communication and computation overheads in large-scale, complex systems [20]. Instead defining agent *neighborhoods* reduces the communication burden, where agents communicate with the agents in their neighborhood; however, determining these neighborhoods is not a trivial task. Poor choices may lead to inefficient communication at best and unsatisfactory control performance at worst. The neighborhoods can be determined from a system dynamics model, if a suitably accurate model is available. However, identifying such a model can be expensive and time consuming. Recently, direct data-driven control methods that avoid model identification have gained traction [9] [4] [12]. However, it is unclear, under the data-driven setting, how to design adequate and yet efficient communication topology.

1.2 Literature Review

Typical distributed control problems take the communication topology to be a constraint rather than a design variable; the System Level Synthesis framework [3] treats controller sparsity structures as a constraint within the distributed control design problem. Distributed model predictive control (MPC) algorithms such as [7] and data-driven distributed MPC schemes [21] [1] assume a known a-priori set of neighbors for each agent. State feedback control in [5] guarantees convergence for an arbitrary communication graph but no information is provided concerning the influence of the topology on the convergence rate.

Previous works addressing communication topology design for control include sparsity-promoting optimal controllers [14] and co-design of topology and distributed controller to balance communication costs against performance [16]. Graph-based methods include community detection [10] and an optimization framework to find stabilizing control structures [24]. We refer to [6] for a detailed survey. These works assume knowledge of the global system model, and provide a basis for this data-driven approach. Recent work [8] uses data-driven methods for network design; this addresses the underlying physical network structure rather than the communication topology of a cyber-layer controller.

1.3 Main Contributions and Paper Structure

We consider a linear time-invariant (LTI) networked system consisting of subsystems coupled through their outputs. The problem we address is to design a communication topology suitable for a distributed control implementation without prior knowledge of a system model. We accomplish this through a centralized optimization problem carried out by a system coordinator, where we collect

persistently exciting data from the global system that can be used to directly synthesize a communication topology and a multi-step output predictor using a least-square prediction error method. We frame our work in the multi-agent setting and take a modular approach such that we only tackle the topology design via the coordinator to set up the control design problem for the individual control agents to analyse; we assume that the topology is (re-)designed on a much slower timescale than control decisions are taken on. We co-optimize predictor and topology within a mixed-integer optimization problem to find a topology that balances communication costs and prediction accuracy and is optimal relative to the specified communication link cost weights. We validate the topology optimization through simulations, showing that prediction cost increases as links are dropped due to greater communication costs, and investigate the connection between the topology design and closed-loop control cost via distributed MPC simulations.

In summary, this paper makes the following original contributions:

- to derive a mixed-integer second-order conic optimization problem (MISOCP) that directly uses data to compute an optimal communication topology and linear predictor and to assess hyperparameter tuning choices.

- to find an upper bound on the prediction error induced by a given topology and the associated error in an open-loop control cost

- to analyse the trade-off between the prediction error and the number of communication links (and the associated communication costs), and the nature of the connection between this trade-off and the realised control cost.

The mathematical formulation of the distributed dynamical system is given in Section 3. In Section 4 we present the mixed-integer conic optimization problem and derive bounds on the prediction error dependent on the chosen topology before simulation results and conclusions are given in Section 5 and Section 6.

2 Preliminaries

We write a T -sample long signal composed of the sequence $\{x(k)\}_{k=1}^T$ in vector form as $x_{[1:T]} = [x^\top(1) \dots x^\top(T)]^\top$. Its Hankel matrix form is defined by:

$$H_N(x) = \begin{bmatrix} x(1) & x(2) & \cdots & x(T-N+1) \\ x(2) & x(3) & \cdots & x(T-N+2) \\ \vdots & \vdots & \ddots & \vdots \\ x(N) & x(N+1) & \cdots & x(T) \end{bmatrix}$$

Definition 1 (Persistency of Excitation). *a signal $x_{[1:T]}$ where $x(k) \in \mathbb{R}^n$ is persistently exciting of order L if $\text{rank}(H_L(x)) = nL$.*

We denote the matrix (block-) diagonal with n (block-) diagonal elements A_i by $\text{diag}\{A_i\}_{i=1}^n$, and use the notation that a matrix A :

$$A = \begin{bmatrix} A_{11} & \cdots & A_{1N_2} \\ \vdots & \ddots & \vdots \\ A_{N_11} & \cdots & A_{N_1N_2} \end{bmatrix}$$

may be represented by $A = \{A_{ij}\}_{i=1:N_1, j=1:N_2}$, and if $N_1 = N_2$ we can write $A = \{A_{ij}\}_{i,j=1:N_1}$. $\mathbb{I}^{a \times b}$ is the identity matrix of dimension $a \times b$, $\mathbf{0}^{a \times b}$ is the zero matrix of dimension $a \times b$ and $\mathbb{1}^{a \times b}$ is a matrix of ones of dimension $a \times b$. $\mathbb{Z}_{>0}$ is the set of positive integers.

3 System Formulation

We consider a set of subsystems $\mathcal{V} = \{1, \dots, M\}$, where M is the total number of subsystems, within a multi-agent cyber-physical system (CPS) framework. Under this approach, we abstract two directed graphs; one for the physical layer, $\mathcal{G}_P = (\mathcal{V}, \mathcal{E}_P)$, and a second for the cyber layer, $\mathcal{G}_C = (\mathcal{V}, \mathcal{E}_C)$, with $\{\mathcal{E}_P, \mathcal{E}_C\} \subseteq \mathcal{V} \times \mathcal{V}$. The physical layer graph represents the physical subsystems and the interconnections between them, whilst the cyber layer graph represents the control agents (one for each subsystem) and the cyber layer communication between the agents. Therefore, both graphs share the same vertex set but have differing edge sets. The edge set \mathcal{E}_P is defined by the physical interconnections between subsystems; i.e., $(j, i) \in \mathcal{E}_P$ if the physical state of subsystem $i \in \mathcal{V}$ is directly influenced by subsystem $j \in \mathcal{V}$. Meanwhile, \mathcal{E}_C is defined by the communication links between agents; $(j, i) \in \mathcal{E}_C$ if agent $j \in \mathcal{V}$ sends information to agent $i \in \mathcal{V}$. We write $\mathcal{N}_i^C = \{j : (j, i) \in \mathcal{E}_C\}$, with \mathcal{N}_i^C denoting the cyber neighborhood of agent i (the set of agents sending information to agent i). The Boolean variable $\delta_{ij} \in \{0, 1\}$ represents whether a communication link exists from agent j to agent i :

$$\delta_{ij} = \begin{cases} 1 & \text{if } (j, i) \in \mathcal{E}_C \\ 0 & \text{otherwise.} \end{cases} \quad (1)$$

There is a cost associated with increasing the total number of communication links due to, e.g., bandwidth limitations, and phenomena such as rapid increases in packet loss when the communication channel utilization threshold is breached [25]. We make a simplifying assumption that each link has a fixed cost.

Assumption 1 *There is a scalar link cost $c_{ij} \in \mathbb{R}_{\geq 0}$ associated with every possible cyber layer edge $(j, i) \in \mathcal{V} \times \mathcal{V}$.*

A typical control problem is to determine the control inputs to minimize some cost as a function of the inputs and outputs of all the agents over a (possibly infinite) time horizon, subject to the system dynamics and without leaving a

feasible region that inputs and/or outputs must stay within. In the multi-agent setting, each agent calculates its control input with a control function $\kappa_i(\cdot)$:

$$u_i(k) = \kappa_i(\xi_i(k), \theta_i, \xi_{\mathcal{N}_i^C}(k), \theta_{\mathcal{N}_i^C}), \quad (2)$$

where designing $\kappa_i(\cdot)$ is the control design problem, θ_i is a vector of local problem parameters such as the weights of the cost of $u_i(k)$ and $y_i(k)$, and $\xi_i(k)$ is an extended state vector of recent local inputs and output measurements (i.e., $\xi_i(k) = [u_i^\top(k-1) \dots u_i^\top(k-N_P) \ y_i^\top(k-1) \dots y_i^\top(k-N_P)]^\top$ for some $N_P \in \mathbb{Z}_{>0}$). Alongside local information θ_i and $\xi_i(k)$, agent i also has information $\theta_{\mathcal{N}_i^C} = \{\theta_j : j \in \mathcal{N}_i^C\}$ and $\xi_{\mathcal{N}_i^C} = \{\xi_j(k) : j \in \mathcal{N}_i^C\}$ from its set of neighboring agents \mathcal{N}_i^C that it can use to improve its decision making and reduce the control cost. We frame our approach with the following problem definition:

Problem 1. Design the cyber layer edge set \mathcal{E}_C with knowledge of the set of subsystems and agents \mathcal{V} , but without knowing the physical layer edge set \mathcal{E}_P .

If two subsystems are physically interconnected, then enabling information sharing between the controlling agents of the subsystems will non-strictly decrease their closed-loop control cost. Stronger interconnections are likely to lead to a greater reduction in cost. Information sharing is enabled by an edge connecting these agents in the cyber layer communication graph.

A distributed LTI system where subsystems are coupled through outputs and outputs are subject to noise may be described by:

$$x_i(k+1) = A_i x_i(k) + B_i u_i(k) + \sum_{j=1}^M E_{ij} y_j(k) \quad (3a)$$

$$y_i(k) = C_i x_i(k) + D_i u_i(k) + v_i(k), \quad (3b)$$

where for subsystem $i \in \mathcal{V}$ and time step k , $x_i(k) \in \mathbb{R}^{n_i}$ is the state, $u_i(k) \in \mathbb{R}^{m_i}$ is the input, $y_i(k) \in \mathbb{R}^{p_i}$ is the output and $v_i(k) \in \mathbb{R}^{p_i}$ is zero-mean white noise. The interconnection matrix $E_{ij} = \mathbf{0}^{n_i \times p_j} \ \forall i = j$. The global system dynamics can be written as:

$$x^{(g)}(k+1) = Ax^{(g)}(k) + Bu^{(g)}(k) \quad (4a)$$

$$y^{(g)}(k) = Cx^{(g)}(k) + Du^{(g)}(k) + v^{(g)}(k), \quad (4b)$$

where the global state, input, output and noise vectors are given by $x^{(g)}(k) = [x_1^\top(k) \dots x_M^\top(k)]^\top$, $u^{(g)}(k) = [u_1^\top(k) \dots u_M^\top(k)]^\top$, $y^{(g)}(k) = [y_1^\top(k) \dots y_M^\top(k)]^\top$ and $v^{(g)}(k) = [v_1^\top(k) \dots v_M^\top(k)]^\top$, respectively. The global state-space matrices in (4) are given by:

$$A = \begin{bmatrix} A_1 & E_{12}C_2 & \dots & E_{1M}C_M \\ E_{21}C_1 & A_2 & \dots & E_{2M}C_M \\ \vdots & \vdots & \ddots & \vdots \\ E_{M1}C_1 & E_{M2}C_2 & \dots & A_M \end{bmatrix}, \quad B = \begin{bmatrix} B_1 & E_{12}D_2 & \dots & E_{1M}D_M \\ E_{21}D_1 & B_2 & \dots & E_{2M}D_M \\ \vdots & \vdots & \ddots & \vdots \\ E_{M1}D_1 & E_{M2}D_2 & \dots & B_M \end{bmatrix} \quad (5a)$$

$$C = \text{diag}\{C_i\}_{i=1}^M, \quad D = \text{diag}\{D_i\}_{i=1}^M, \quad (5b)$$

Assumption 2 *The subsystems in the set \mathcal{V} all follow dynamics (3), and the global physical system made up of the graph \mathcal{G}_P obeys dynamics (4). The pair (A, C) is observable, and the pair (A, B) is controllable. Furthermore, whilst we consider systems obeying the dynamics in (4), we assume that the matrices A_i , B_i , C_i and D_i in (3) are unknown $\forall i \in \mathcal{V}$, and E_{ij} is unknown $\forall j \in \mathcal{V}$, $j \neq i$.*

Due to Assumption 2, we use a central coordinator to generate an input signal $u_{[1:T]}^{(g),d}$ that obeys Assumption 3 to excite the dynamics; resulting output measurements allow an understanding of system behavior. The superscript d denotes collected data used in topology design.

Assumption 3 ([9] Lemmas 4.1 and 4.2) *For $\{T_{ini}, N\} \in \mathbb{Z}_{>0}$, the signal $u_{[1:T]}^{(g),d} \in \mathbb{R}^{m^{(g)}T}$ is persistently exciting of order $T_{ini} + N + n^{(g)}$; $m^{(g)} = \sum_{i=1}^M m_i$ and $n^{(g)} = \sum_{i=1}^M n_i$. T is chosen such that $T \geq (m^{(g)} + 1)(T_{ini} + N + n^{(g)}) - 1 = T_{min}$, and $T_{ini} \geq \ell$, where ℓ is the system lag (that is, the smallest integer such that the observability matrix $[C^\top (CA)^\top \dots (CA^{\ell-1})^\top]^\top$ has rank $n^{(g)}$).*

The corresponding collected output signal is given by $y_{[1:T]}^{(g),d} \in \mathbb{R}^{p^{(g)}T}$, with $p^{(g)} = \sum_{i=1}^M p_i$. The collected input and output data may be written as Hankel matrices $U^{(g),d} = H_{T_{ini}+N}(u_{[1:T]}^{(g),d})$, $Y^{(g),d} = H_{T_{ini}+N}(y_{[1:T]}^{(g),d})$. We permute and partition these matrices to end up with four subsystem-ordered data matrices:

$$U^P = \begin{bmatrix} U_1^P \\ \vdots \\ U_M^P \end{bmatrix}, \quad Y^P = \begin{bmatrix} Y_1^P \\ \vdots \\ Y_M^P \end{bmatrix}, \quad U^F = \begin{bmatrix} U_1^F \\ \vdots \\ U_M^F \end{bmatrix}, \quad Y^F = \begin{bmatrix} Y_1^F \\ \vdots \\ Y_M^F \end{bmatrix} \quad (6)$$

where $\forall i \in \mathcal{V}$: $U_i^P = H_{T_{ini}}(u_{i[1:T-N]}^d)$, $Y_i^P = H_{T_{ini}}(y_{i[1:T-N]}^d)$, $U_i^F = H_N(u_{i[N+1:T]}^d)$, $Y_i^F = H_N(y_{i[N+1:T]}^d)$, and the Hankel matrices are dimensioned by $U^P \in \mathbb{R}^{T_{ini}m^{(g)} \times (T - (T_{ini} + N) + 1)}$, $Y^P \in \mathbb{R}^{T_{ini}p^{(g)} \times (T - (T_{ini} + N) + 1)}$, $U^F \in \mathbb{R}^{Nm^{(g)} \times (T - (T_{ini} + N) + 1)}$ and $Y^F \in \mathbb{R}^{Np^{(g)} \times (T - (T_{ini} + N) + 1)}$. Note we have separated the first T_{ini} from the remaining N block rows of the Hankel matrices.

If there is zero noise, the data matrix $[U^{(g),d^\top} Y^{(g),d^\top}]^\top$ will span the subspace of trajectories of length $T_{ini} + N$ if it has rank $Nm^{(g)} + n^{(g)}$ [23]. This result forms the cornerstone of the behavioral control methods [9] [4] and is aligned with the Subspace Predictive Control (SPC) approach [15]. The SPC methodology is based on subspace identification and makes use of a linear output predictor:

$$\hat{y}^{(g)} = K \begin{bmatrix} u_{ini}^{(g)} \\ y_{ini}^{(g)} \\ u_f^{(g)} \end{bmatrix}, \quad (7)$$

where $u_{ini}^{(g)} \in \mathbb{R}^{m^{(g)}T_{ini}}$ and $y_{ini}^{(g)} \in \mathbb{R}^{p^{(g)}T_{ini}}$ are the initialization trajectories (most recent T_{ini} inputs and outputs) $u_f^{(g)} \in \mathbb{R}^{m^{(g)}N}$ is the future N -step input

sequence and $y_f^{(g)} \in \mathbb{R}^{p^{(g)}N}$ is the N -step output prediction trajectory. $K \in \mathbb{R}^{p^{(g)}N \times (m^{(g)}+p^{(g)})T_{ini}+m^{(g)}N}$ is the predictor matrix. In Section 4 below, we will examine a standard least-norm optimization problem to determine K before including the influence of the communication topology within the prediction. First, we make a final assumption building on Assumption 2 to ensure the existence of a stabilizing control law for the designed topology.

Assumption 4 *The parameters of the global system dynamics defined by (4) are such that the global system does not have any unstable decentralized fixed modes (DFMs) [11], hence there exists a decentralized control law (i.e., when $\delta_{ij} = 0 \forall \{i, j\} \in \mathcal{V}$) that results in a stable closed-loop system response; i.e., each subsystem can stabilize itself despite the coupling with neighbors.*

Note that each agent i has access to the local information u_i and y_i required for a decentralized control implementation where $u_i(k) = \kappa_i(\theta_i, \xi_i(k))$ without communication, hence Assumption 4 holds if there are no unstable DFMs.

4 Communication Topology and Predictor Optimization

Traditional control approaches consist of a two-stage procedure of first estimating a parametric model of the system to be controlled before designing a controller to stabilize/steer the model according to the desired behavior, often with a third intermediate step to design a state estimator with the model. The SPC approach [15] instead identifies a predictor of future system behavior using least-squares regression, which can then be used in an explicit control law to determine the optimal input sequence.

4.1 Least-Squares Predictor Identification

A similar prediction error method (PEM) that is combined with MPC [19] finds an optimal linear predictor that is used in the MPC optimization problem; this is formulated as a bi-level optimization. The predictor is found by considering each column in the Hankel matrices (6) as a trajectory; we can use (7) to make

a prediction \hat{Y}^F of Y^F ; $\hat{Y}^F = K \begin{bmatrix} U^P \\ Y^P \\ U^F \end{bmatrix}$. The predictor K optimizing the least-squares fitting criterion is found as the minimizer of [13]:

$$\min_{\hat{K}} \left\| Y^F - \hat{K} \begin{bmatrix} U^P \\ Y^P \\ U^F \end{bmatrix} \right\|_F^2 \quad (8a)$$

$$\text{s.t. } \hat{K} = [\hat{K}_p^u \ \hat{K}_p^y \ \hat{K}_f] \quad (8b)$$

$$\text{rank}([\hat{K}_p^u \ \hat{K}_p^y]) = n^{(g)} \quad (8c)$$

$$\hat{K}_f \text{ Lower-Block Triangular,} \quad (8d)$$

where the rank constraint ensures LTI dynamics of order $n^{(g)}$ and the lower-block triangular constraint ensures causality in predictions. Supposing Assumptions 2 and 3 hold, then the Hankel data matrices (6) in (8) span the trajectory subspace [9] and K calculated with (8) is able to accurately predict an output trajectory according to (7). When data is noise-free, an exact closed-form solution exists and is given by Y^F multiplied by the pseudo-inverse of the concatenated remaining Hankel matrices (i.e., $K = Y^F \left[U^{P^\top} \ Y^{P^\top} \ U^{F^\top} \right]^\top$) as the solution to the unconstrained least squares problem.

4.2 Including the Communication Costs in Predictor Optimization

We now consider the desire to minimize communication costs defined by Eq. (1) and supposing Assumption 1 holds; i.e., $\min_{\{\delta_{ij}\}_{i,j=1:M}} \sum_{i,j=1}^M c_{ij} \delta_{ij}$ with the set of Boolean δ_{ij} variables defining \mathcal{E}_C . Consider that if $\delta_{ij} = 0$, there is no link transferring information from agent j to agent i , therefore agent i 's predictions cannot be calculated using the measurements or decisions of agent j . By writing K as:

$$K = \begin{bmatrix} K_{p,11}^u & \cdots & K_{p,1M}^u & K_{p,11}^y & \cdots & K_{p,1M}^y & K_{f,11} & \cdots & K_{f,1M} \\ \vdots & \ddots & \vdots & \vdots & \ddots & \vdots & \vdots & \ddots & \vdots \\ K_{p,M1}^u & \cdots & K_{p,MM}^u & K_{p,M1}^y & \cdots & K_{p,MM}^y & K_{f,M1} & \cdots & K_{f,MM} \end{bmatrix}, \quad (9)$$

the communication topology influence on predictor structure is encoded by $\delta_{ij} = 0 \implies [K_{p,ij}^u \ K_{p,ij}^y \ K_{f,ij}] = 0$. We seek to choose the edge set \mathcal{E}_C that minimizes communication costs and least-square prediction error by optimizing over $\delta_{ij} \forall \{i, j\} \in \mathcal{V}$ and \hat{K} within a multi-criteria mixed-integer program:

$$\min_{\Delta, \hat{K}} \sum_{i,j=1}^M c_{ij} \delta_{ij} + \left\| Y^F - \hat{K} \begin{bmatrix} U^P \\ Y^P \\ U^F \end{bmatrix} \right\|_F^2 \quad (10a)$$

$$\text{s.t. } \delta_{ij} \in \{0, 1\} \quad \forall \{i, j\} \in \mathcal{V} \quad (10b)$$

$$\Delta = \{\delta_{ij}\}_{i,j=1:M} \quad (10c)$$

$$\hat{K} = [\hat{K}_p^u \ \hat{K}_p^y \ \hat{K}_f] \quad (10d)$$

$$\text{rank}([\hat{K}_p^u \ \hat{K}_p^y]) = n^{(g)} \quad (10e)$$

$$\hat{K}_f \text{ Lower-Block Triangular} \quad (10f)$$

$$\hat{K}_p^u = \{\hat{K}_{p,ij}^u\}_{i,j=1:M}, \ \hat{K}_p^y = \{\hat{K}_{p,ij}^y\}_{i,j=1:M}, \ \hat{K}_f = \{\hat{K}_{f,ij}\}_{i,j=1:M} \quad (10g)$$

$$\delta_{ij} = 0 \implies [\hat{K}_{p,ij}^u \ \hat{K}_{p,ij}^y \ \hat{K}_{f,ij}] = 0 \quad \forall \{i, j\} \in \mathcal{V}, \ i \neq j. \quad (10h)$$

In order to solve (10), we first perform a convex relaxation and drop the rank (10e) and causality (10f) constraints. Our approach is to increase the data trajectory length T and average over multiple datasets to reduce the effect of noise and implicitly the need for the rank constraint. Ensuring a causal predictor

structure is beneficial but not a strict requirement for predictive control, see [13]; non-causal predictors can still achieve acceptable performance. Next, we perform a convex big-M relaxation [16] on the implication constraint (10h); that is, we replace it with:

$$\left. \begin{aligned} -\overline{M}\delta_{ij}\mathbb{1}^{p_i N \times m_j T_{\text{ini}}} &\leq \hat{K}_{p,ij}^u \leq \overline{M}\delta_{ij}\mathbb{1}^{p_i N \times m_j T_{\text{ini}}} \\ -\overline{M}\delta_{ij}\mathbb{1}^{p_i N \times p_j T_{\text{ini}}} &\leq \hat{K}_{p,ij}^f \leq \overline{M}\delta_{ij}\mathbb{1}^{p_i N \times p_j T_{\text{ini}}} \\ -\overline{M}\delta_{ij}\mathbb{1}^{p_i N \times m_j N} &\leq \hat{K}_{f,ij} \leq \overline{M}\delta_{ij}\mathbb{1}^{p_i N \times m_j N} \end{aligned} \right\} \forall \{i, j\} \in \mathcal{V}, i \neq j. \quad (11)$$

This relaxation ensures (10h) holds both when $\delta_{ij} = 0$, and when $\delta_{ij} = 1$ assuming that all elements of \hat{K} are bounded by $-\overline{M} \leq \hat{K}_{ij} \leq \overline{M}$. The choice of \overline{M} should be as small as possible to improve solver efficiency but large enough that it does not constrain the predictor sub-matrices from giving accurate predictions. We arrive at a mixed-integer quadratic program:

$$\min_{\Delta, \hat{K}} \sum_{i,j=1}^M c_{ij} \delta_{ij} + \left\| Y^F - \hat{K} \begin{bmatrix} U^P \\ Y^P \\ U^F \end{bmatrix} \right\|_F^2 \quad (12a)$$

$$\text{s.t. } \delta_{ij} \in \{0, 1\} \quad \forall \{i, j\} \in \mathcal{V} \quad (12b)$$

$$\Delta = \{\delta_{ij}\}_{i,j=1:M} \quad (12c)$$

$$\hat{K} = [\hat{K}_p^u \quad \hat{K}_p^y \quad \hat{K}_f] \quad (12d)$$

$$\hat{K}_p^u = \{\hat{K}_{p,ij}^u\}_{i,j=1:M}, \quad \hat{K}_p^y = \{\hat{K}_{p,ij}^y\}_{i,j=1:M}, \quad \hat{K}_f = \{\hat{K}_{f,ij}\}_{i,j=1:M} \quad (12e)$$

$$\left. \begin{aligned} -\overline{M}\delta_{ij}\mathbb{1}^{p_i N \times m_j T_{\text{ini}}} &\leq \hat{K}_{p,ij}^u \leq \overline{M}\delta_{ij}\mathbb{1}^{p_i N \times m_j T_{\text{ini}}} \\ -\overline{M}\delta_{ij}\mathbb{1}^{p_i N \times p_j T_{\text{ini}}} &\leq \hat{K}_{p,ij}^f \leq \overline{M}\delta_{ij}\mathbb{1}^{p_i N \times p_j T_{\text{ini}}} \\ -\overline{M}\delta_{ij}\mathbb{1}^{p_i N \times m_j N} &\leq \hat{K}_{f,ij} \leq \overline{M}\delta_{ij}\mathbb{1}^{p_i N \times m_j N} \end{aligned} \right\} \forall \{i, j\} \in \mathcal{V}, i \neq j, \quad (12f)$$

which may be represented as an MISOCP. Whilst this can take significant computation to solve for very large systems, we note that the communication topology is designed offline therefore computational efficiency is of reduced importance compared to an online algorithm.

In the case of noisy data, the solution to problem (12) may give very low prediction error due to overfitting to the noise as we have dropped the rank constraint (10e). A common approach to get around this issue is to collect $N_{\text{coll}} \in \mathbb{Z}_{>0}$ datasets using exactly the same input sequence, and then average the Hankel matrices obtained from the N_{coll} experiments [19]. Since the noise is assumed to be zero-mean, the effect is to remove the noise from the data. The online measurements used to make predictions (e.g., in (7)) will also be subject to noise; estimators such as the extended Kalman filter for output-feedback behavioral control [2] may be used to deal with this issue. Application of such approaches is outside the scope of this work as we focus on optimality of the communication topology and associated predictor and do not address online control. Supposing Assumption 4 holds, then a stabilizing control law exists for the optimized K .

4.3 Bounding the Prediction Error

By considering the case where the communication graph is fully connected, we can deduce a bound on the prediction error when links are dropped. Intuitively, we expect that a graph with more links will lead to a lower prediction error; Theorem 1 shows that the topology optimization scheme (12) is consistent with this and that the prediction cost of (12) under the optimized topology is bounded by the cost of the dropped links. We will use this to find an upper bound on the open-loop prediction error induced by dropping links. Adding a constraint that $\delta_{ij} = 1 \forall \{i, j\} \in \mathcal{V}$, $i \neq j$ leads to (12) simplifying to an unconstrained optimization, assuming that \bar{M} is sufficiently large:

$$\min_{\hat{K}} J(\hat{K}) = \min_{\hat{K}} \sum_{i,j=1, i \neq j}^M c_{ij} + \left\| Y^F - \hat{K} \begin{bmatrix} U^P \\ Y^P \\ U^F \end{bmatrix} \right\|_F^2. \quad (13)$$

We denote a minimizer of (13) by K' , and the value the cost function of (13) evaluated at the minimizer by $J'(K')$. The topology-predictor pair minimizing (12) is given by (Δ^*, K^*) , and the cost function evaluation at this minimizer is denoted as $J(\Delta^*, K^*)$, with $\Delta^* = \{\delta_{ij}^*\}_{i,j=1:M}$.

Theorem 1. *Considering the t -th column of Y^F as an N -step output trajectory y_f^t of (4) and the t -th column of \hat{Y}^F to be a prediction \hat{y}_f^t of y_f^t where $1 \leq t \leq T - (T_{ini} + N) + 1$, the sum of the Euclidean norm of the trajectory prediction errors $\sum_{t=1}^{T-(T_{ini}+N)+1} \|y_f^t - \hat{y}_f^t\|_2^2$ induced by a given optimized topology Δ^* and predictor K^* is lower bounded by the prediction error with a fully connected communication graph equal to $\|Y^F(I - \Pi)\|_F^2$, where $\Pi = \begin{bmatrix} U^P \\ Y^P \\ U^F \end{bmatrix}^\dagger \begin{bmatrix} U^P \\ Y^P \\ U^F \end{bmatrix}$, and upper bounded by the sum of this lower bound with the sum of the communication costs of the links not included in the optimized topology, equal to $\|Y^F(I - \Pi)\|_F^2 + \sum_{i,j=1, i \neq j}^M c_{ij}(1 - \delta_{ij}^*)$.*

Proof. We write $J(\Delta^*, K^*) = \sum_{i,j=1}^M c_{ij} \delta_{ij}^* + \left\| Y^F - K^* \begin{bmatrix} U^P \\ Y^P \\ U^F \end{bmatrix} \right\|_F^2$. Since $\Delta_1 = \{\delta_{ij}\}_{i,j=1:M}$ where $\delta_{ij} = 1 \forall \{i, j\} \in \mathcal{V}$, $i \neq j$ is a feasible topology for (12), which has a feasible optimal predictor K' when \bar{M} is sufficiently large, (Δ_1, K') is a feasible solution of (12). Therefore $J(\Delta^*, K^*) \leq J(\Delta_1, K') = J'(K')$, so $J(\Delta^*, K^*) - J'(K') \leq 0$:

$$\sum_{i,j=1}^M c_{ij} \delta_{ij}^* - \sum_{i,j=1, i \neq j}^M c_{ij} + \left\| Y^F - K^* \begin{bmatrix} U^P \\ Y^P \\ U^F \end{bmatrix} \right\|_F^2 - \left\| Y^F - K' \begin{bmatrix} U^P \\ Y^P \\ U^F \end{bmatrix} \right\|_F^2 \leq 0. \quad (14)$$

Optimization (13) is unconstrained and the communication costs do not affect the location of the minimum, hence K' is a global minimizer of $J'(\hat{K})$ and the

least-square prediction error given by $K' = Y^F \begin{bmatrix} U^P \\ Y^P \\ U^F \end{bmatrix}^\dagger$. This naturally leads to:

$$\left\| Y^F \left(I - \begin{bmatrix} U^P \\ Y^P \\ U^F \end{bmatrix}^\dagger \begin{bmatrix} U^P \\ Y^P \\ U^F \end{bmatrix} \right) \right\|_F^2 = \|Y^F(I - \Pi)\|_F^2 \leq \left\| Y^F - K^* \begin{bmatrix} U^P \\ Y^P \\ U^F \end{bmatrix} \right\|_F^2. \quad (15)$$

Considering the Frobenius norm as the sum of the 2-norm of the matrix columns (with each column a trajectory and a prediction respectively in the left and right matrix evaluations inside the Frobenius norm), from (14) we find:

$$\sum_{t=1}^{T-(T_{\text{ini}}+N)+1} \|y_f^t - \hat{y}_f^t\|_2^2 \leq \sum_{i,j=1, i \neq j}^M c_{ij}(1 - \delta_{ij}^*) + \|Y^F(I - \Pi)\|_F^2. \quad (16)$$

Note we can always set $\delta_{ii} = 0 \forall i \in \mathcal{V}$ without influencing prediction accuracy. Applying the same consideration to (15) gives:

$$\|Y^F(I - \Pi)\|_F^2 \leq \sum_{t=1}^{T-(T_{\text{ini}}+N)+1} \|y_f^t - \hat{y}_f^t\|_2^2, \quad (17)$$

providing the upper and lower bounds on the total prediction error over all the samples in the collected dataset as desired. Note that the lower bound evaluates to zero when data is noise-free as exact predictions may be found. \square

Whilst bounds on the overall prediction error induced by a given topology are informative, it is useful to have bounds on the error for an individual trajectory prediction as would be used in solving a control problem.

Lemma 1. *Consider a control output penalty term for a regulation problem of the form $\|y_f\|_Q^2$ where $Q \succeq 0$ is a weighting matrix. The error in the open-loop prediction cost, given by $\|y_f - \hat{y}_f\|_Q^2$, is bounded by $\lambda_{Q, \max}(\sum_{i,j=1, i \neq j}^M c_{ij}(1 - \delta_{ij}^*) + \|Y^F(I - \Pi)\|_F^2)$, where $\lambda_{Q, \max}$ is the largest eigenvalue of Q .*

Proof. A worst-case bound on any individual trajectory y_f is found from (16) as:

$$\|y_f - \hat{y}_f\|_2^2 \leq \sum_{i,j=1, i \neq j}^M c_{ij}(1 - \delta_{ij}^*) + \|Y^F(I - \Pi)\|_F^2. \quad (18)$$

We can write $Q = V_Q \Lambda_Q V_Q^\top$ since Q is symmetric, where V_Q is a matrix of eigenvectors of Q and Λ_Q is a matrix of its eigenvalues. Let $y_f - \hat{y}_f = V_Q \tilde{y}$, then $\|y_f - \hat{y}_f\|_Q^2 = \tilde{y}^\top V_Q^\top V_Q \Lambda_Q V_Q^\top V_Q \tilde{y} = \tilde{y}^\top \Lambda_Q \tilde{y}$ since $V_Q^\top = V_Q^{-1}$. Note that

$\|y_f - \hat{y}_f\|_2^2 = \tilde{y}^\top V_Q^\top V_Q \tilde{y} = \tilde{y}^\top \tilde{y}$ and $\tilde{y}^\top A_Q \tilde{y} \leq \lambda_{Q,\max} \tilde{y}^\top \tilde{y}$, therefore $\|y_f - \hat{y}_f\|_Q^2 \leq \lambda_{Q,\max} \|y_f - \hat{y}_f\|_2^2$. Combining this fact with (18) gives the result:

$$\|y_f - \hat{y}_f\|_Q^2 \leq \lambda_{Q,\max} \left(\sum_{i,j=1, i \neq j}^M c_{ij} (1 - \delta_{ij}^*) + \|Y^F (I - \Pi)\|_F^2 \right). \quad (19)$$

□

This upper bound gives the worst-case output prediction weighted according to the control weight matrix Q ; however, it is likely to be rather conservative. We next present simulation results using (12) where we optimize communication topology and predictor and observe that the open-loop prediction cost error, bounded by Lemma 1, does indeed correlate with closed-loop control cost.

5 Simulations

We use the linearized and discretized swing dynamics as given in [1] for topology optimization and control simulations. Each subsystem has dynamics (3), with $x_i(k) = [\theta_i(k) \ \omega_i(k)]^\top$, $B_i = [0 \ \frac{1}{m_i}]^\top$, $C_i = [1 \ 0]$, $D_i = \mathbf{0}^{p_i \times m_i}$ and the matrices A_i and E_{ij} are given by:

$$A_i = \begin{bmatrix} 1 & \Delta t \\ -\frac{k_i}{m_i} \Delta t & 1 - \frac{d_i}{m_i} \Delta t \end{bmatrix} \quad E_{ij} = \begin{bmatrix} 0 \\ \frac{k_{ij}}{m_i} \Delta t \end{bmatrix}, \quad (20)$$

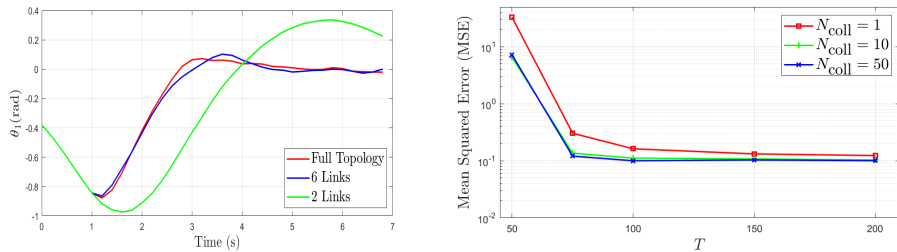
where θ_i and ω_i represent phase angle and frequency deviations, and m_i , d_i and k_{ij} represent inertia, damping and coupling for each subsystem, with the time step given by $\Delta t = 0.2$ and $k_i = \sum_{j=1/i}^M k_{ij}$. We choose $M = 4$, $m_1 = 1.4$, $m_2 = 0.8$, $m_3 = 0.6$, $m_4 = 0.9$, $d_1 = 0.6$, $d_2 = d_4 = 0.65$, $d_3 = 0.75$, $k_{12} = k_{21} = 1.25$, $k_{23} = k_{32} = 1.2$, $k_{34} = k_{43} = 0.075$, $k_{13} = k_{14} = k_{24} = k_{31} = k_{41} = k_{42} = 0$. A persistently exciting input signal $u_{[1:T]}^{(g),d}$ was created using a pseudo-randomly generated sequence of zero-mean normally distributed numbers with variance $\sigma_d^2 = 1$ and injected into the test system within MATLAB simulations. The collected output data $y_{[1:T]}^{(g),d}$ and input $u_{[1:T]}^{(g),d}$ form the data Hankel matrices (6) in order to solve (12). We choose $T_{\text{ini}} = 3$, $N = 5$, and $\bar{M} = 5$. Following tuning described below, T and N_{coll} were chosen as 200 and 50, respectively.

The optimization (12) is solved in MATLAB using GUROBI [17] with the YALMIP toolbox [22], and we use an identical link cost $c_{ij} = c \ \forall \{i, j\} \in \mathcal{V}$. We test prediction accuracy and assess if overfitting to noise is occurring by injecting a random signal (each element sampled from a zero-mean normal distribution with variance σ_d^2) into each subsystem and calculating the mean-squared error (MSE) of predictions compared to true (denoised) outputs. Results for an SNR of 10^3 averaged over 50 trials are presented in Table 1, giving the adjacency matrix for \mathcal{G}_C , optimization prediction cost and prediction MSE for different communication costs. Links are first dropped between subsystems that are uncoupled before links between coupled subsystems are dropped. Results show that

Table 1: Optimization results with an SNR of 10^3 , showing that links are dropped as the communication cost grows, resulting in increasing prediction cost and MSE

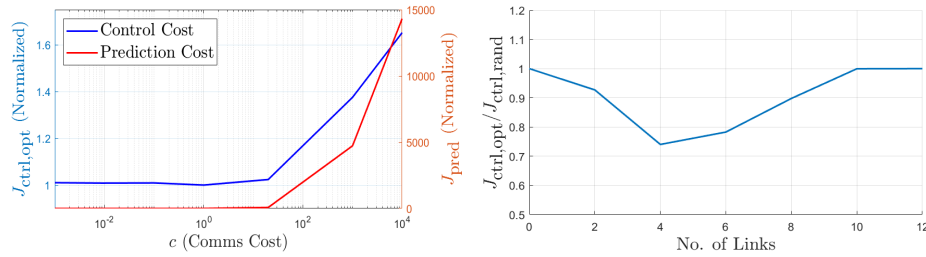
c	# Links	Topology	Pred. Cost	MSE
0.001	12	$\begin{bmatrix} 0 & 1 & 1 & 1 \\ 1 & 0 & 1 & 1 \\ 1 & 1 & 0 & 1 \\ 1 & 1 & 1 & 0 \end{bmatrix}$	0.31	0.100
1	6	$\begin{bmatrix} 0 & 1 & 0 & 0 \\ 1 & 0 & 1 & 0 \\ 0 & 1 & 0 & 1 \\ 0 & 0 & 1 & 0 \end{bmatrix}$	0.68	0.119
20	4	$\begin{bmatrix} 0 & 1 & 0 & 0 \\ 1 & 0 & 1 & 0 \\ 0 & 1 & 0 & 0 \\ 0 & 0 & 0 & 0 \end{bmatrix}$	16.73	0.457
1000	2	$\begin{bmatrix} 0 & 0 & 0 & 0 \\ 0 & 0 & 1 & 0 \\ 0 & 1 & 0 & 0 \\ 0 & 0 & 0 & 0 \end{bmatrix}$	1034.71	1.247

half the links can be dropped before significant prediction errors occur; note that there are 6 couplings (non-zero k_{ij}) out of a possible maximum of 12. Our approach is to reduce the effects of noise by averaging over N_{coll} datasets and using a $T > T_{\text{min}}$. We investigate varying these hyperparameters to provide sufficient performance without unduly large computational burdens. Results averaged over 500 trials based on an all-to-all topology are shown in Figure 1b. MSE converges as T and N_{coll} increase; we choose $T = 200$ and $N_{\text{coll}} = 50$ to benefit both topology optimization and data-driven control algorithms.



(a) Evolution of θ_1 for all-to-all communication and optimized topologies with 2 and 6 links (b) MSE decreases with increasing T and N_{coll} (results for an SNR of 10^3)

Fig. 1: Simulation results for (a) no noise and (b) tuning T and N_{coll}



(a) Control cost and prediction cost from topology optimization are closely correlated (b) Ratio of control cost for optimized topologies and a random topology with the same number of links

Fig. 2: Control simulation results showing (a) control cost $J_{ctrl,opt}$ and prediction cost J_{pred} for optimized topologies and (b) the ratio of $J_{ctrl,opt}$ to random topology control cost $J_{ctrl,rand}$

Finally, we investigate the influence of topology choice on control cost and its correlation with prediction cost using test system (20). Control is implemented using a non-cooperative data-driven MPC scheme based on [21] with a minor extension using slack variables, similarly to [9], to guarantee feasibility and stability with measurement noise. Output trajectories for θ_1 shown in Figure 1a for 3 optimized topologies. There is a clear correlation between prediction cost of the topology optimization and closed-loop control cost, shown in Figure 2a, in accordance with our approach to use prediction cost as a metric for topology optimality. Note the significant difference in growth rate of control and prediction costs. The control cost for an optimized topology consistently outperforms a random topology, shown in Figure 2b; topologies with both 0 and 12 links cannot be random so these costs are equal. There is a maximum reduction of around 25 % in control cost for the optimized topology compared to the average random topology. This demonstrates the capability of the scheme to find an effective communication topology for distributed control.

6 Conclusions and Outlook

We have proposed a fully data-driven method for optimizing the communication topology of distributed control schemes via an MISOCP for LTI cyber-physical systems that do not have any unstable DFMs, assuming knowledge of a persistently exciting input sequence of sufficient order. The prediction cost under the optimized topology is upper bounded by the sum of the link costs not included in the topology with the prediction cost under all-to-all communication. Simulations demonstrated that the optimized topology achieves low prediction error up to a threshold where prediction accuracy decreases as further links are dropped. Control simulations showed that the prediction cost of the topology optimization is correlated with realized control cost, and demonstrated reductions in control cost using the optimized topology compared to a random topology. Future work aims to improve scalability via distributed optimization, further analyse the

connection between prediction cost and closed-loop control cost, and investigate data-driven methods to guarantee stability when unstable DFMs exist.

References

1. Alonso, C.A., Yang, F., Matni, N.: Data-driven distributed and localized model predictive control. *IEEE Open J. of Control Syst.* 1, 29–40 (2022)
2. Alpagó, D., Dörfler, F., Lygeros, J.: An extended kalman filter for data-enabled predictive control. *IEEE Control Syst. Lett.* 4(4), 994–999 (2020)
3. Anderson, J., Doyle, J.C., Low, S.H., Matni, N.: System level synthesis. *Annu. Rev. Control* 47, 364–393 (2019)
4. Berberich, J., Köhler, J., Müller, M.A., Allgöwer, F.: Data-driven model predictive control with stability and robustness guarantees. *IEEE Trans. Autom. Control* 66, 1702–1717 (2019)
5. Celi, F., Baggio, G., Pasqualetti, F.: Distributed data-driven control of network systems. *IEEE Open J. of Control Syst.* pp. 1–15 (2023)
6. Chanfreut, P., Maestre, J.M., Camacho, E.F.: A survey on clustering methods for distributed and networked control systems. *Annu. Rev. Control* 52, 75–90 (2021)
7. Conte, C., Jones, C.N., Morari, M., Zeilinger, M.N.: Distributed synthesis and stability of cooperative distributed model predictive control for linear systems. *Automatica* 69, 117–125 (2016)
8. Coraggio, M., di Bernardo, M.: Data-driven design of complex network structures to promote synchronization. arXiv preprint, submitted to *IEEE Control Syst. Lett.* and 2023 American Control Conf. (ACC) (09 2023)
9. Coulson, J., Lygeros, J., Dörfler, F.: Data-enabled predictive control: In the shallows of the deepc. In: 2019 18th Eur. Control Conf. (ECC). pp. 307–312 (06 2019)
10. Daoutidis, P., Tang, W., Jogwar, S.S.: Decomposing complex plants for distributed control: Perspectives from network theory. *Computers & Chem. Eng.* 114, 43–51 (2018), fOCAPO/CPC 2017
11. Davison, E., Özgüner, U.: Characterizations of decentralized fixed modes for interconnected systems. *Automatica* 19(2), 169–182 (1983)
12. De Persis, C., Tesi, P.: Formulas for data-driven control: Stabilization, optimality, and robustness. *IEEE Trans. Autom. Control* 65(3), 909–924 (2020)
13. Dörfler, F., Coulson, J., Markovskiy, I.: Bridging direct and indirect data-driven control formulations via regularizations and relaxations. *IEEE Trans. Autom. Control* 68(2), 883–897 (2023)
14. Dörfler, F., Jovanović, M.R., Chertkov, M., Bullo, F.: Sparsity-promoting optimal wide-area control of power networks. *IEEE Trans. Power Syst.* 29(5), 2281–2291 (2014)
15. Favoreel, W., Moor, B.D., Gevers, M.: Spc: Subspace predictive control. *IFAC Proceedings Volumes* 32(2), 4004–4009 (1999), 14th IFAC World Congress 1999, Beijing, Chia, 5-9 July
16. Groß, D., Stursberg, O.: Optimized distributed control and network topology design for interconnected systems. In: 2011 50th IEEE Conf. on Decision and Control and Eur. Control Conf. pp. 8112–8117 (2011)
17. Gurobi Optimization, LLC: Gurobi Optimizer Reference Manual (2023), <https://www.gurobi.com>
18. Han, X., Heussen, K., Gehrke, O., Bindner, H.W., Kroposki, B.: Taxonomy for evaluation of distributed control strategies for distributed energy resources. *IEEE Trans. Smart Grid* 9(5), 5185–5195 (2018)

19. Huang, L., Coulson, J., Lygeros, J., Dörfler, F.: Data-enabled predictive control for grid-connected power converters. In: 2019 IEEE 58th Conf. on Decision and Control (CDC). pp. 8130–8135 (2019)
20. Jovanović, M.R., Dhingra, N.K.: Controller architectures: Tradeoffs between performance and structure. *Eur. J. of Control* 30, 76–91 (2016), 15th Eur. Control Conf., ECC16
21. Kohler, M., Berberich, J., Müller, M.A., Allgower, F.: Data-driven distributed mpc of dynamically coupled linear systems. *IFAC-PapersOnLine* 55(30), 365–370 (2022), 25th Int. Symp. on Math. Theory of Networks and Syst. MTNS 2022
22. Löfberg, J.: Yalmip : A toolbox for modeling and optimization in matlab. In: Proceedings of the CACSD Conf. Taipei, Taiwan (2004)
23. Markovsky, I., Dörfler, F.: Behavioral systems theory in data-driven analysis, signal processing, and control. *Annu. Rev. Control* 52, 42–64 (2021)
24. Mosalli, H., Babazadeh, M.: Stabilizing control structures: An optimization framework. *IEEE Trans. Autom. Control* 67(7), 3738–3745 (2022)
25. Wu, D., Nie, X., Asmare, E., Arkhipov, D.I., Qin, Z., Li, R., McCann, J.A., Li, K.: Towards distributed sdn: Mobility management and flow scheduling in software defined urban iot. *IEEE Trans. Parallel and Distributed Syst.* 31(6), 1400–1418 (2020)